Run-by-Run Process Control of Metal Sputter Deposition: Combining Time Series and Extended Kalman Filter

Juhn-Horng Chen, Tzu-Wei Kuo, and An-Chen Lee, *Member, IEEE*

***Abstract*—By the time series model, this paper constructed the disturbance model for the aluminum sputter deposition process and derived the extending Kalman filter (EKF) controller based on this new disturbance model. Experimental results reveal that ARI(3,1) model appropriately characterizes the dynamic behavior of the disturbance for the processes. The EKF controller which includes information of process noise and measurement noise is able to regulate the model coefficients automatically as the target is replaced or degrades. In this paper, the d-EWMA controller, time-varying d-EWMA controller, age-based d-EWMA controller, and EKF controller have been applied to aluminum sputter deposition processes for predicting deposition rates and comparing their performances. The application of the EKF controller here is proven to improve the estimating accuracy of the aluminum sputter deposition process significantly, regardless of whether the deposition rates are measured at each run or not.**

***Index Terms*—d-EWMA controller, deposition rate, extended Kalman filter, time series model, time-varying d-EWMA controller.**

I. INTRODUCTION

COMPUTER INTEGRATED MANUFACTURING (CIM), which enhances the management and production process efficiency of a factory, is an important development trend for manufacturing upgrade. Advanced process control (APC) has been recognized as a proper tool for maximizing profitability of semiconductor manufacturing facilities by improving efficiency and product quality. Currently, run-by-run model-based process control (RbR MBPC) methods with good quality and reliability performance for APC application are most applicable.

Spanos *et al.* [1] describes a statistical process control (SPC) scheme that takes advantage of such real-time information for generating malfunction alarms but not for prescribing control action. Sachs *et al.* [2] proposes a modular framework for implementing process control to the LPCVD of polysilicon in very large-scale integration (VLSI) fabrication. The system which takes both the preceding and following processes into consideration integrates existing approaches with new methodologies in order to achieve online optimization and control of unit process. Sachs *et al.* [3] provides a framework which combines SPC and feedback control for controlling processes affected by disturbances such as shifts and drifts. Additionally, the run-by-run controller is implemented and tested by applications to a silicon epitaxy process in a barrel reactor. In the work of Sachs *et al.* [3], the process is assumed to have no dynamics and a linear controller based on the exponentially weighted moving average (EWMA) is in use. The performance of this approach is highly dependent on the choice of the EWMA controller parameters (EWMA weights) and the ability to dynamically update the EWMA weight. Several authors [4]–[6] address this problem in their studies and propose the self-tuning EWMA controller which dynamically updates its controller parameters. An EWMA controller is effective for slowly drifting processes but is insufficient for processes with large drifts. Many extensions of the EWMA controller, such as the predictor–corrector controller (PCC) [7], [8], double-EWMA (d-EWMA) controller [9], age-based double-EWMA controller [10], and time-varying d-EWMA controller [11] are developed for large drifting processes.

Metal sputter deposition for semiconductor manufacturing benefits greatly by RbR MBPC [12]. In particular, sputter deposition experiences a characteristic drift in the deposition rate which occurs in all processes. In this paper, we will first review the d-EWMA, time-varying d-EWMA, and age-based d-EWMA controllers. By using the time series model, we will then construct the disturbance model of the aluminum sputter deposition process and derive the extending Kalman filter (EKF) controller based on the disturbance model. The proposed EKF controller which is capable of simultaneously estimating the deposition rate and updating model parameters is applied to aluminum sputter deposition processes for predicting the deposition rates and comparing its performance with other methods. Experimental results reveal that applying the EKF controller here significantly improves the performance of the estimator of the aluminum sputter deposition process, no matter the deposition rates are measured at each run or not.

II. RBR CONTROLLERS OF METAL SPUTTER DEPOSITION PROCESS

A basic diagram of metal sputter deposition is shown in Fig. 1. Ions are discharged from plasma which dislodges particles from the metal sputter target for keeping a desired deposition thickness of wafers. Maintaining a desired thickness is difficult because metal sputter deposition processes are characterized by

Manuscript received March 26, 2006; revised March 28, 2007. This work was supported by the National Science Council of the Republic of China under Contract NSC94-2218-E-009-002.

J.-H. Chen is with the Department of Mechanical Engineering, Chung Hua University, Hsinchu 300, Taiwan, R.O.C. (e-mail: chen@chu.edu.tw).

T.-W. Kuo and A.-C. Lee are with the Department of Mechanical Engineering, National Chiao-Tung University, Hsinchu 300, Taiwan, R.O.C. (e-mail: ypk.me94g@nctu.edu.tw; aclee@mail.nctu.edu.tw).

Digital Object Identifier 10.1109/TSM.2007.901392

0894-6507/$25.00 © 2007 IEEE

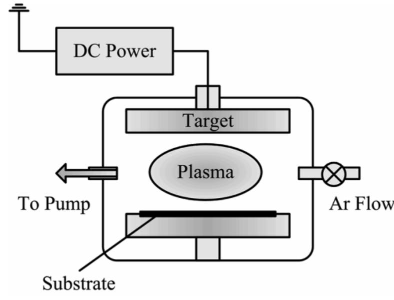

Fig. 1. Metal sputter process diagram.

decreasing deposition rate as the sputter target degrades. Variation in the gas flows, vacuum pressure, process temperature, dc power, and molecular uniformity of the sputter target contribute various amounts of variation in the measured deposition rate in addition to the characteristic drift which occurs from wafer to wafer. The drifting nature of metal sputter deposition makes it necessary to change the process recipe continually for compensating the drift. An appropriate model for metal sputter deposition is of the form [12]

$$\mathrm{Rate}[k] = \mathrm{Rate}[0] + \varepsilon[k] \tag{1}$$

where $\mathrm{R}[0]$ is the deposition rate at the beginning of the target life and $\varepsilon[k]$ is the error in the deposition rate (from Rate[0]) on run k, which may be due to the degradation of the sputter target and the uncertain factors, such as changes in the gas flows, vacuum pressure, etc. Here, one would like to obtain the updated deposition rate and then make changes to the deposition time (process recipe) on every run. In this paper, one considers two particular implementations of this strategy, referred to as RbR MBPC (run-by-run model-based process control).

The first implementation of an RbR MBPC strategy is referred to here as the double-exponential weight moving average (d-EWMA) controllers including time-varying weights. Guo *et al.* [9] shows that, for the semiconductor manufacturing processes with random shifts and drifts, the d-EWMA method is better than the EWMA and the PCC methods. The d-EWMA controller defines the process drift from run $(k-1)$ to run k as

$$p[k-1] = \varepsilon[k] - \varepsilon[k-1]. \tag{2}$$

The d-EWMA controller is summarized as the following equations:

$$\begin{aligned}\hat{\varepsilon}[k \mid k] &= w_1(\mathrm{Rate_m}[k] - \hat{\mathrm{Rate}}[0]) \\ &\quad + (1-w_1)(\hat{\varepsilon}[k-1 \mid k-1] + \hat{p}[k-1 \mid k-1])\end{aligned} \tag{3}$$

$$\begin{aligned}\hat{p}[k \mid k] &= w_2(\mathrm{Rate_m}[k] - \hat{\mathrm{Rate}}[0] - \hat{\varepsilon}[k-1 \mid k-1]) \\ &\quad + (1-w_2)\hat{p}[k-1 \mid k-1]\end{aligned} \tag{4}$$

$$\hat{\varepsilon}[k+1 \mid k] = \hat{\varepsilon}[k \mid k] + \hat{p}[k \mid k] \tag{5}$$

where $\mathrm{Rate_m}[k]$ denotes the measurement of the deposition rate on run k.

Su and Hsu [11] proposed a time-varying weights tuning method of d-EWMA controller. The tuning method is summarized in the following equations:

$$w_1[k] = \max\{w_1, w_2\} \tag{6}$$

$$w_2[k] = \min\{w_1, w_2\} + (f)^k \tag{7}$$

where f $(0 \le f < 1)$ expresses the discount factor.

The estimated rate on run $(k+1)$ is

$$\hat{\mathrm{Rate}}[k+1 \mid k] = \hat{\mathrm{Rate}}[0] + \hat{\varepsilon}[k+1 \mid k]. \tag{8}$$

The process time on run $(k+1)$ is then computed as follows:

$$\text{Process Time}[k+1] = \frac{\text{Desired Thickness}}{\text{Estimated Rate}} = \frac{\text{Desired Thickness}}{\hat{\mathrm{Rate}}[k+1 \mid k]}. \tag{9}$$

The second implementation of an RbR MBPC strategy is the aged-based d-EWMA controller. In many applications, the deposition rate is not measured at each run. This leads to an invalid result in the d-EWMA formula. However, the data collected often comes with an indication of the run number. Chen and Guo [10] propounded an age-based d-EWMA controller and utilized the process time to modify the drifting term to deal with unequally spacing measurements. If the kth and $(k+d)$th deposition rates are measured but the rates from the $(k+1)$th to the $(k+d)$th runs are unmeasured, the correction equations on run k are the same as (3) and (4), but the prediction equation becomes

$$\hat{\varepsilon}[k+n \mid k] = \hat{\varepsilon}[k \mid k] + n \cdot \hat{p}[k \mid k], \quad n = 1, 2, \ldots, d. \tag{10}$$

The estimated rates and the process time from $(k+1)$ to $(k+d)$ runs are

$$\hat{\mathrm{Rate}}[k+n \mid k] = \hat{\mathrm{Rate}}[0] + \hat{\varepsilon}[k+n \mid k], \quad n = 1, 2, \ldots, d \tag{11}$$

$$\text{Process Time}[k+n] = \frac{\text{Desired Thickness}}{\text{Estimated Rate}} = \frac{\text{Desired Thickness}}{\hat{\mathrm{Rate}}[k+n \mid k]}, \quad n = 1, 2, \ldots, d. \tag{12}$$

Once the rate on run $(k+d)$ is measured, the correction equations then becomes

$$\begin{aligned}\hat{\varepsilon}[k+d \mid k+d] &= w_1(\mathrm{Rate_m}[k+d] - \hat{\mathrm{Rate}}[0]) \\ &\quad + (1-w_1)(\hat{\varepsilon}[k \mid k] + d \cdot \hat{p}[k \mid k])\end{aligned} \tag{13}$$

$$\begin{aligned}\hat{p}[k+d \mid k+d] &= w_2\left(\frac{\mathrm{Rate_m}[k+d] - \hat{\mathrm{Rate}}[0] - \hat{\varepsilon}[k \mid k]}{d}\right) \\ &\quad + (1-w_2)\hat{p}[k \mid k].\end{aligned} \tag{14}$$

In this paper, we contemplate the aluminum sputter processes on an Applied Materials Endura in Powerchip Semiconductor Corporation. The sputter tool has two chambers (chamber 2 and chamber 3) for the aluminum process with desired deposition thicknesses spanning a range of 4000 Å. The sputter target will be replaced when the dc energy accumulation reaches 1600 KWH. Consider the historical data for process deposition rate with a constant dc power shown in Fig. 2. Here, the characteristic of drift in the deposition rate is caused by the degradation of target over the long term (in kilowatt-hours). As illustrated in Fig. 2, it appears that the rate at which the process

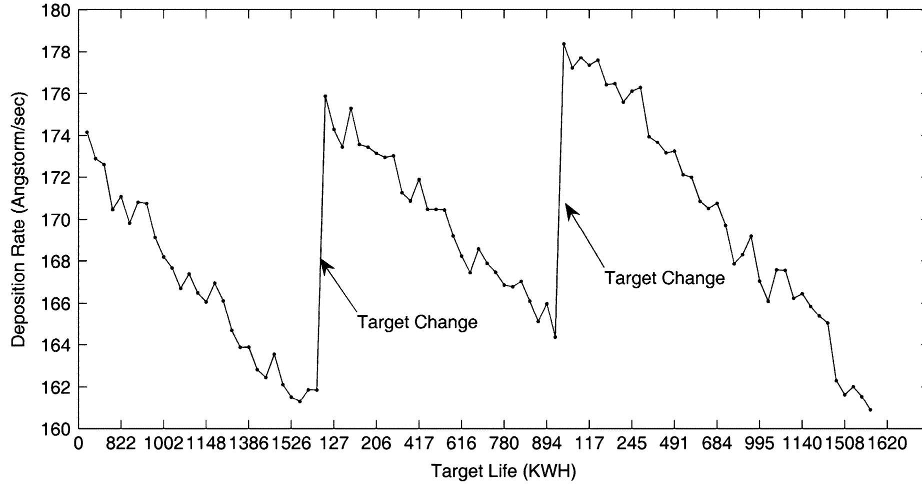

Fig. 2. Historical data of aluminum deposition rate.

drifts varies from target to target. Box and Jenkins [13] show that a controller based on the EWMA statistic is a minimum mean square error (MMSE) controller when the underlying process disturbance follows the IMA(1,1) (first-order integrated moving average) process. However, from Fig. 2, one is not sure whether the error $\varepsilon[k]$ or the process drift $p[k]$ follows an IMA(1,1) process. To ascertain the dynamic behavior of the deposition rate further, one will model the error $\varepsilon[k]$ by an autoregressive integrated moving average (ARIMA) (p,d,q) process [13]

$$\phi(B)\nabla^d\varepsilon[k] = \theta_0 + \theta(B)a[k] \tag{15}$$

where

$$\begin{aligned}\phi(B) &= 1 - \phi_1 B - \phi_2 B^2 \cdots - \phi_p B^p\\ \theta(B) &= 1 - \theta_1 B - \theta_2 B^2 \cdots - \theta_q B^q\\ \nabla &= 1 - B\end{aligned}$$

where B is the backshift operator and $a[k]$: is the white noise.

By using historical data to fit the time series model [13], one obtains the disturbance model in the following form:

$$(1 - \phi_1 B - \phi_2 B^2 - \phi_3 B^3)(1 - B)\varepsilon[k] = \theta_0 + a[k] \tag{16}$$

or

$$(1 - \phi_1 B - \phi_2 B^2 - \phi_3 B^3)p[k-1] = \theta_0 + a[k] \tag{17}$$

or

$$\begin{aligned}\varepsilon[k] &= (1+\phi_1)\varepsilon[k-1] + (\phi_2 - \phi_1)\varepsilon[k-2]\\ &\quad + (\phi_3 - \phi_2)\varepsilon[k-3] - \phi_4\varepsilon[k-4] + \theta_0 + a[k].\end{aligned} \tag{18}$$

The disturbance $\varepsilon[k]$ is an ARI(3,1) process and the process drift $p\,[k]$ is an AR(3) process. The estimate of the process drift is

$$\begin{aligned}E[p[k-1]] &= E[\varepsilon[k] - \varepsilon[k-1]]\\ &= E[(1-B)\varepsilon[k]] = \frac{\theta_0}{1 - \phi_1 - \phi_2 - \phi_3}.\end{aligned}$$

Since the rate of the process drifts varies from target to target, forecasting the disturbance and updating the coefficients of the disturbance model $(\phi_1, \phi_2, \phi_3, \theta_0)$ for different target are essential. Define the process state $\mathrm{X}[k]$ as

$$\begin{aligned}\mathbf{X}[k] &= \{x_1[k], x_2[k], \ldots, x_8[k]\}^T\\ &= \{\varepsilon[k], \varepsilon[k-1], \varepsilon[k-2], \varepsilon[k-3],\\ &\qquad \phi_1[k], \phi_2[k], \phi_3[k], \theta_0[k]\}^T.\end{aligned}$$

Thus, (18) can be written as in (19), shown at the bottom of the page, with the corresponding measurement model

$$\begin{aligned}&\mathrm{Rate_m}[k+1] - \hat{\mathrm{R}}\mathrm{ate}[0]\\ &\quad = [1,0,0,0,0,0,0,0]\,\mathbf{X}[k+1] + v[k+1]\\ &\quad = \mathbf{H}\mathbf{X}[k+1] + v[k+1]\end{aligned} \tag{20}$$

$$\mathbf{X}[k+1] = \begin{bmatrix}(1+x_5[k])x_1[k] + (x_6[k] - x_5[k])x_2[k] + (x_7[k] - x_6[k])x_3[k] - x_7[k]x_4[k] + x_8[k]\\ x_1[k]\\ x_2[k]\\ x_3[k]\\ x_5[k]\\ x_6[k]\\ x_7[k]\\ x_8[k]\end{bmatrix} + \begin{bmatrix}a[k+1]\\0\\0\\0\\0\\0\\0\\0\end{bmatrix} = \mathbf{F}(\mathbf{X}[k]) + \mathbf{a}[k+1] \tag{19}$$

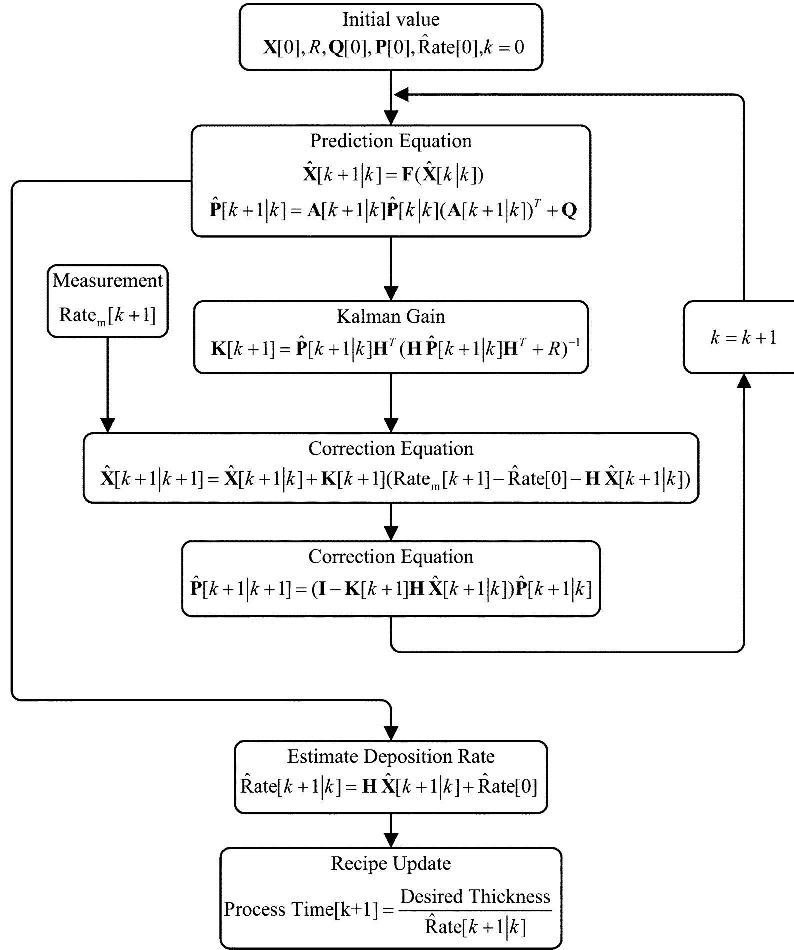

Fig. 3. Block diagram of EKF controller.

where $v[k]$ is the measurement noise. Also, the process noise, measurement noise, and process state have the properties

$$E[\mathbf{a}[k]\mathbf{a}^T[j]] = \mathbf{Q}\delta_{\rm kj} \quad \mathbf{Q} \geq 0, \quad \forall k, j \geq 0$$
$$E[v[k]v^T[j]] = R\delta_{\rm kj}, \quad R \geq 0, \quad \forall k, j \geq 0$$
$$E[v[k]\mathbf{X}[k]] = \mathbf{0} \quad \forall k \geq 0.$$

Thus, the $(k+1)$th state and state covariance ($\hat{\mathbf{X}}[k+1\,|\,k]$ and $\hat{\mathbf{P}}[k+1\,|\,k]$) can be predicted by the discrete extended Kalman filter (EKF) [14] algorithm

$$\hat{\mathbf{X}}[k+1\,|\,k] = \mathbf{F}(\hat{\mathbf{X}}[k\,|\,k]) \tag{21}$$
$$\hat{\mathbf{P}}[k+1\,|\,k] = \mathbf{A}[k+1\,|\,k]\hat{\mathbf{P}}[k\,|\,k](\mathbf{A}[k+1\,|\,k])^T + \mathbf{Q}. \tag{22}$$

The correction equations are

$$\hat{\mathbf{X}}[k+1\,|\,k+1] = \hat{\mathbf{X}}[k+1\,|\,k] + \mathbf{K}[k+1](\mathrm{Rate_m}[k+1] - \hat{\mathrm{R}}\mathrm{ate}[0] - \mathbf{H}\hat{\mathbf{X}}[k+1\,|\,k]) \tag{23}$$
$$\hat{\mathbf{P}}[k+1\,|\,k+1] = (\mathbf{I} - \mathbf{K}[k+1]\mathbf{H}\hat{\mathbf{X}}[k+1\,|\,k])\hat{\mathbf{P}}[k+1\,|\,k] \tag{24}$$

and the Kalman gain is

$$\mathbf{K}[k+1] = \hat{\mathbf{P}}[k+1\,|\,k]\mathbf{H}^T(\mathbf{H}\hat{\mathbf{P}}[k+1\,|\,k]\mathbf{H}^T + R)^{-1} \tag{25}$$

where the matrix A is the Jacobian matrix and is defined as shown at the bottom of the next page. When the $(k+1)$th state $\hat{\varepsilon}[k+1\,|\,k]$ is estimated, the estimated rate and the process time on run $(k+1)$ is then computed by (8) and (9). A block diagram of the EKF controller is shown in Fig. 3.

If the deposition rate is not measured at each run, the EKF controller is able to be extended easily. Suppose the deposition rate from the $(k+1)$th to the $(k+d)$th measurements are unmeasured, the prediction (21)–(22) are modified as

$$\hat{\mathbf{X}}[k+n+1\,|\,k] = \mathbf{F}(\hat{\mathbf{X}}[k+n\,|\,k]), \quad n = 0, 1, 2, \ldots, d-1 \tag{26}$$
$$\hat{\mathbf{P}}[k+n+1\,|\,k] = \mathbf{A}[k+n+1\,|\,k]\hat{\mathbf{P}}(k+n\,|\,k)(\mathbf{A}[k+n+1\,|\,k])^T + \mathbf{Q}, \quad n = 0, 1, 2, \ldots, d-1. \tag{27}$$

The estimated rates and the process time from $(k+1)$ to $(k+d)$ runs are then obtained from (11)–(12). Once the deposition rate on run $(k+d)$ is measured, the correction equations are

$$\hat{\mathbf{X}}[k+d\,|\,k+d] = \hat{\mathbf{X}}[k+d\,|\,k] + \mathbf{K}[k+d](\mathrm{Rate_m}[k+d] - \hat{\mathrm{R}}\mathrm{ate}[0] - \mathbf{H}\,\hat{\mathbf{X}}[k+d\,|\,k]) \tag{28}$$

$$\hat{\mathbf{P}}[k+d\,|\,k+d] = (\mathbf{I}-\mathbf{K}[k+d]\mathbf{H}\,\hat{\mathbf{X}}[k+d\,|\,k])\hat{\mathbf{P}}[k+d\,|\,k] \quad (29)$$

and the Kalman gain is

$$\mathbf{K}[k+d] = \hat{\mathbf{P}}[k+d\,|\,k]\mathbf{H}^T(\mathbf{H}\hat{\mathbf{P}}[k+d\,|\,k]\mathbf{H}^T+R)^{-1}. \quad (30)$$

III. Experimental Results and Discussion

In this section, the d-EWMA, the time-varying d-EWMA, the age-based d-EWMA, and the EKF controllers were applied to the aluminum sputter process to estimate the deposition rates and compare their performances. In all cases the power setting is fixed. The historical data of the eight targets with equally spacing measurement are used for verifying the performance of the controllers. All targets are not at the beginning of target life. The first four history data is for comparing the abilities of the d-EWMA, the time-varying d-EWMA, and the EKF controllers, and the other is for comparing the abilities of the age-based d-EWMA and the EKF controllers. The choice of weights, w_1 and w_2, for the d-EWMA, time-varying d-EWMA, and the age-based d-EWMA controllers, is critical for achieving optimal performance. Different weights are carried out from the first target for d-EWMA and time-varying d-EWMA controllers, and the fifth target for age-based d-EWMA controller; the values which bring the smallest mean square error (MSE) $w_1 = w_2 = 0.6$ for the d-EWMA controller, $w_1 = w_2 = 0.6, f = 0.032$ for the time-varying d-EWMA controller, and $w_1 = 0.69, w_2 = 0.98$ for the age-based d-EWMA controller are adopted. MSE is defined as

$$\mathrm{MSE} = \frac{\sum_{k=1}^{n}[\mathrm{Rate_m}[k]-\hat{\mathrm{Rate}}[k]]^2}{n}. \quad (31)$$

As for the EKF, the initial conditions, such as the disturbance and the coefficients of the disturbance model ($\hat{\mathrm{X}}[0]$), the covariance matrices of the state, and the process noise ($\hat{P}[0\,|\,0]$ and Q), are acquired from the first target. The initial deposition rate ($\hat{\mathrm{Rate}}[0]$) is obtained from the mean of the initial values of eight targets. The covariance of the measurement noise (R) is obtained from the instrument manual. The initial conditions and the covariance of the measurement noise are listed in the Appendix.

For all controllers, the initial estimates are reset to the initial conditions when the target is changed. The deposition rates estimated by the d-EWMA and the EKF controllers with the measured deposition rates for each run are shown in Fig. 4. For target 3, the initial estimate of the deposition rate is lower than the actual one since it is the youngest target of all. It appears that the deposition rates estimated by both controllers still track the actual one instantaneously. Table I illustrates the MSE values of deposition rates by various controllers and the percentages of improvement by the EKF controller. It is evident that the EKF controller reduces the MSE significantly. Additionally, when the optimal weights of d-EWMA controller based on target 2 are employed ($w_1 = w_2 = 0.1$) and the initial conditions of the EKF controller remain the same as before, the estimation results are shown in Table II where the EKF controller still demonstrates superior estimation performance. This phenomenon validates that the ARI (3,1) model for exhibiting the dynamic behavior of the disturbance is more appropriate than two IMA(1,1) models used in d-EWMA. In addition, in contrast to d-EWMA which requires us to specify its model coefficients (weights), the EKF controller involves the information of the process noise and the measurement noise and regulates the model coefficients automatically, which is essential for improving the performance of the estimator.

TABLE I
MSE of Estimated Deposition Rates for EKF, d-EWMA, and Time-Varying d-EWMA Controllers With Equal Spacing Data

MSE(Å/s)^2	Target #1	Target #2	Target #3	Target #4
d-EWMA	1.13725	1.12579	1.39385	1.76262
time-varying d-EWMA	1.13292	1.14302	1.41064	1.6944
EKF	0.93298	0.7048	1.19417	1.03466
Improvement (%) over d-EWMA	12%	37%	14%	41%
Improvement (%) over time-varying d-EWMA	12%	39%	15%	39%

TABLE II
MSE of Estimated Deposition Rates for EKF and d-EWMA Controllers Based on Target 2 With Equal Spacing Data

MSE(Å/s)^2	Target #1	Target #2	Target #3	Target #4
d-EWMA	2.1409	0.71783	2.1472	1.5714
EKF	0.93298	0.7048	1.19417	1.03466
Improvement (%) over d-EWMA	56%	2%	44%	34%

$$\mathbf{A}[k] = \left(\frac{\partial\mathbf{F}(\mathbf{X}[k])}{\partial\mathbf{X}[k]}\right)^T = \begin{bmatrix} 1+x_5[k] & x_6[k]-x_5[k] & x_7[k]-x_6[k] & -x_7[k] & 0 & 0 & 0 & 1 \\ 1 & 0 & 0 & 0 & 0 & 0 & 0 & 0 \\ 0 & 1 & 0 & 0 & 0 & 0 & 0 & 0 \\ 0 & 0 & 1 & 0 & 0 & 0 & 0 & 0 \\ 0 & 0 & 0 & 0 & 1 & 0 & 0 & 0 \\ 0 & 0 & 0 & 0 & 0 & 1 & 0 & 0 \\ 0 & 0 & 0 & 0 & 0 & 0 & 1 & 0 \\ 0 & 0 & 0 & 0 & 0 & 0 & 0 & 1 \end{bmatrix}$$

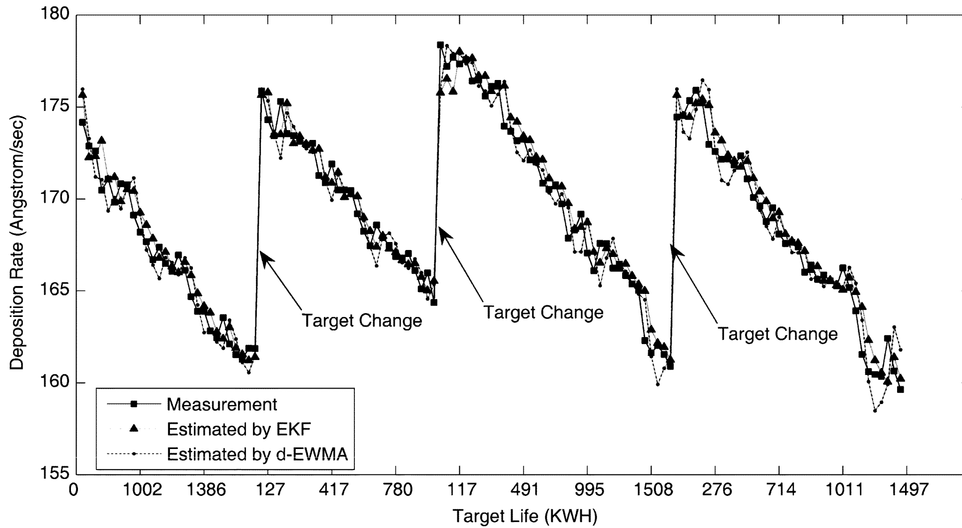

Fig. 4. Estimated deposition rates with equally spacing data.

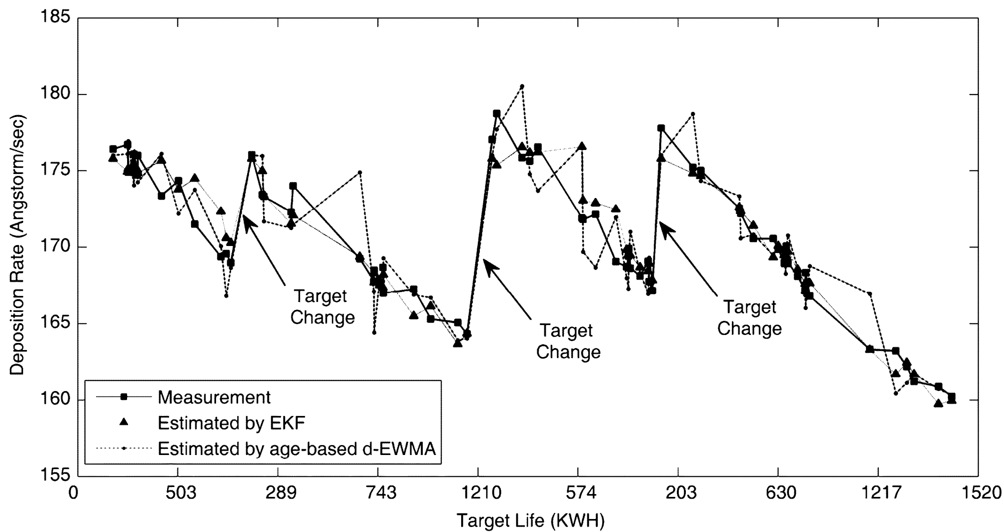

Fig. 5. Estimated deposition rates with unequal spacing data.

In Fig. 5, the deposition rates generated by omitting some measurements of the last four historical data by the EKF controller and age-based d-EWMA controllers are illustrated with the unequal spacing measurements. The MSE values of deposition rates of both controllers and the percentages of the MSE improved by the EKF controller are presented in Table III. It is evident that the EKF controller reduces the MSE significantly. Consider (10), the age-based d-EWMA controller based on the assumption of the constant drift $(\hat{p}[k \mid k])$ utilizes the number of the unmeasured run to modify the drifting term. However, the process drift follows an AR(3) process [see (16)]. The assumption that drift follows an IMA(1,1) process in age-based d-EWMA will result in a large error. In order to investigate the dynamic behavior of the drift thoroughly, assume that the deposition rates of first 25 runs of target 3 are measured and perform deposition rate estimation by d-EWMA and EKF controllers. Then, assume the deposition rates from runs 26 to 35 are unmeasured and perform deposition rate estimation by age-based d-EWMA and EKF controllers. The estimates together

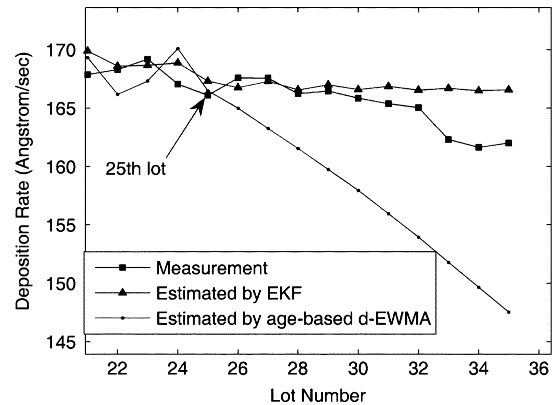

Fig. 6. Estimated deposition rates when measurements, run 26 to 35 of target 3, are not measured.

with measurements from run 26 to 35 are shown in Fig. 6. Fig. 6 demonstrates that the EKF controller is more appropriate than

TABLE III
MSE OF ESTIMATED DEPOSITION RATES FOR AGE-BASED D-EWMA AND EKF CONTROLLERS WITH UNEQUAL SPACING DATA

MSE(Å/s)^2	Target #5	Target #6	Target #7	Target #8
age-based d-EWMA	3.17630	5.03984	5.71981	2.63959
EKF	2.52976	1.04607	3.17804	0.69125
Improvement (%) over age-based EWMA	26%	79%	44%	74%

$$\hat{\mathbf{P}}[0 \mid 0] = \begin{bmatrix} 3.3581\times10^{-4} & 1.1793\times10^{-5} & 1.2943\times10^{-5} & 1.2734\times10^{-5} & -6.6768\times10^{-8} & -7.3242\times10^{-8} & -7.2085\times10^{-8} & 1.3011\times10^{-5} \\ 1.1793\times10^{-5} & 2.3031 & 0.059512 & 0.13506 & -0.013049 & -3.33713\times10^{-4} & -7.6523\times10^{-4} & 0.029059 \\ 1.2943\times10^{-5} & 0.059512 & 1.8623 & 0.038299 & -3.33713\times10^{-4} & -0.010551 & -2.1696\times10^{-4} & 0.031876 \\ 1.2734\times10^{-5} & 0.13506 & 0.038299 & 1.8845 & -7.6523\times10^{-4} & -2.1695\times10^{-4} & -0.010677 & 0.031372 \\ -6.6768\times10^{-8} & -0.013049 & -3.33713\times10^{-4} & -7.6523\times10^{-4} & 7.3934\times10^{-5} & 1.9101\times10^{-6} & 4.3357\times10^{-6} & -1.6446\times10^{-4} \\ -7.3242\times10^{-8} & -3.33713\times10^{-4} & -0.010551 & -2.1695\times10^{-4} & 1.9101\times10^{-6} & 5.9783\times10^{-5} & 1.2292\times10^{-6} & -1.806\times10^{-4} \\ -7.2085\times10^{-8} & -7.6523\times10^{-4} & -2.1696\times10^{-4} & -0.010677 & 4.3357\times10^{-6} & 1.2292\times10^{-6} & 6.0497\times10^{-5} & -1.7775\times10^{-4} \\ 1.3011\times10^{-5} & 0.029059 & 0.031876 & 0.031372 & -1.6446\times10^{-4} & -1.806\times10^{-4} & -1.7775\times10^{-4} & 0.032084 \end{bmatrix}$$

$$\mathbf{Q} = \begin{bmatrix} 0.8281 & 0 & 0 & 0 & 0 & 0 & 0 & 0 \\ 0 & 0 & 0 & 0 & 0 & 0 & 0 & 0 \\ 0 & 0 & 0 & 0 & 0 & 0 & 0 & 0 \\ 0 & 0 & 0 & 0 & 0 & 0 & 0 & 0 \\ 0 & 0 & 0 & 0 & 0 & 0 & 0 & 0 \\ 0 & 0 & 0 & 0 & 0 & 0 & 0 & 0 \\ 0 & 0 & 0 & 0 & 0 & 0 & 0 & 0 \\ 0 & 0 & 0 & 0 & 0 & 0 & 0 & 0 \end{bmatrix}$$

$$\hat{\mathbf{X}}[0] = \begin{bmatrix} \varepsilon[0] \\ \varepsilon[-1] \\ \varepsilon[-2] \\ \varepsilon[-3] \\ \phi_1[0] \\ \phi_2[0] \\ \phi_3[0] \\ \theta_0[0] \end{bmatrix} = \begin{bmatrix} 176.4597 \\ 56.6671 \\ 64.7412 \\ 19.343 \\ -0.32472 \\ -0.27825 \\ -0.11767 \\ -0.10732 \end{bmatrix}$$

$$R = 0.003359362$$

$$\hat{\text{R}}\text{ate}[0] = 176.4597\ (\text{Å/sec})$$

the age-based d-EWMA controller when the deposition rates are unmeasured.

IV. CONCLUSION

In this paper, the EKF controller from the time series model is obtained, which is formed by the history data of the aluminum sputter deposition process. Experimental results reveal that, for the aluminum sputter processes, the ARI(3,1) model characterizes the dynamic behavior of the disturbance appropriately. The EKF controller possesses the ability to regulate the model coefficients automatically as the target is replaced or degrades. Furthermore, its weight (Kalman gain) is self-tuning and includes the information of the process noise and measurement noise. For predicting the deposition rates and comparing their performances, the d-EWMA, time-varying d-EWMA, and EKF controllers have been applied to aluminum sputter deposition processes. If the deposition rate can be measured on each run, these methods have the function to track for process drifts but EKF provides a more accurate rate estimator (25% improvement in average over d-EWMA and 26% improvement in average over time-varying d-EWMA). We have outlined how the EKF controller can be modified to estimate the deposition rate when the rate cannot be measured on each run. The application of the EKF controller result here significantly improves 55% over the aged-based d-EWMA controller, while the deposition rates are not measured on each run.

APPENDIX

Initial Conditions and covariance of the measurement noise is shown in the equations found at the top of the page.

REFERENCES

[1] C. J. Spanos, H. F. Guo, A. Miller, and J. Levine-Parrill, "Real-time statistical process control using tool data," *IEEE Trans. Semicond. Manuf.*, vol. 5, no. 4, pp. 308–318, Nov. 1992.

[2] E. Sachs, R. S. Guo, S. Ha, and A. Hu, "Process control system for VSLI fabrication," *IEEE Trans. Semicond. Manuf.*, vol. 4, no. 2, pp. 134–144, May 1991.

[3] E. Sachs, A. Hu, and A. Ingolfsson, "Run by run process control: Combining SPC and feedback control," *IEEE Trans. Semicond. Manuf.*, vol. 8, no. 1, pp. 26–43, Feb. 1995.

[4] T. H. Smith and D. S. Boing, "A self-tuning EWMA controller utilizing artificial neural network function approximation techniques," *IEEE Trans. Compon. Packag. Manuf. Technol. C*, vol. 20, no. 2, pp. 121–132, Apr. 1997.

[5] R. S. Guo, J. J. Chen, A. Chen, and S. S. Lu, "A self-tuning run-by-run process controller for processes subject to random disturbances," *J. Chin. Inst. Eng.*, vol. 22, no. 5, pp. 627–638, Sep. 1999.

[6] S. T. Tseng, A. B. Yeh, F. Tsung, and Y. Y. Chan, "A study of variable EWMA controllers," *IEEE Trans. Semicond. Manuf.*, vol. 16, no. 4, pp. 633–643, Nov. 2003.

[7] S. W. Butler and J. A. Stefani, "Supervisory run-to-run control of polysilicon gate etch using *in situ* ellipsometry," *IEEE Trans. Semicond. Manuf.*, vol. 7, no. 2, pp. 193–201, May 1994.

[8] L. Sattler and P. E. Hecker, "Reducing cost and increasing throughput using model-based process control on sputtering systems," in *Proc. IEEE/CPMT Int. Electronics Manufacturing Technology Symp.*, Oct. 1998, pp. 409–414.

[9] R. S. Guo, A. Chen, and J. J. Chen, "Run-to-run control schemes for CMP process subject to deterministic drifts," in *Proc. Semiconductor Manufacturing Technology Workshop*, Hsinchu, R.O.C., 2000, pp. 251–258.

[10] A. Chen and R. S. Guo, "Age-based double EWMA controller and its application to CMP process," *IEEE Trans. Semicond. Manuf.*, vol. 14, no. 1, pp. 11–19, Feb. 2001.

[11] C. T. Su and C. C. Hsu, "A time-varying weights tuning method of the double EWMA controller," *Omega-Int. J. Manage. S.*, vol. 32, no. 6, pp. 473–480, Mar. 2004.

[12] T. H. Smith, D. S. Boning, J. Stefani, and S. W. Butler, "Run by run advanced process control of metal sputter deposition," *IEEE Trans. Semicond. Manuf.*, vol. 11, no. 2, pp. 276–284, May 1998.

[13] G. E. P. Box, G. M. Jenkins, and G. C. Reinsel, *Time Series Analysis Forecasting and Control*, 3rd ed. Englewood Cliffs, NJ: Prentice-Hall, 1994.

[14] A. Corigliano and S. Mariani, "Parameter identification in explicit structural dynamics: Performance of the extend Kalman filter," *Comput. Method. Appl. M.*, vol. 193, pp. 3807–3835, Sep. 2004.

Juhn-Horng Chen was born in Taipei, Taiwan, R.O.C., in 1960. He received the B.S. degree in mechanical engineering from National Cheng-Kung University, Tainan, Taiwan, R.O.C., in 1983, and the M.S. and Ph.D. degrees in mechanical engineering from National Chiao-Tung University, Hsinchu, Taiwan, R.O.C., in 1988 and 1994.

He is currently an Associate Professor at Chung-Hua University, Hsinchu, Taiwan, R.O.C. His research interests include advanced process control, chaotic systems and control, and rotor dynamics.

Tzu-Wei Kuo was born in Taoyuan, Taiwan, R.O.C., in 1977. He received the B.S. and M.S. degrees in mechanical engineering from Chung-Hua University, Hsinchu, Taiwan, R.O.C., in 2001 and 2005, respectively. He is currently working toward the Ph.D. degree in mechanical engineering from National Chiao-Tung University, Hsinchu, Taiwan.

His research interests include run-to-run control and process control.

An-Chen Lee (M'04) was born in Chiayi, Taiwan, R.O.C., in 1956. He received the B.S. and M.S. degrees in power mechanical engineering from National Tsing-Hua University, Hsinchu, Taiwan, R.O.C., and the Ph.D. degree in mechanical engineering from University of Wisconsin, Madison, in 1986.

From 1986 to 1990, he was an Associate Professor with the Department of Mechanical Engineering, National Chiao-Tung University, Hsinchu, Taiwan, R.O.C., where he is currently a Professor. He is also the Vice President of National Formosa University, Yunlin, Taiwan. At National Chiao-Tung University, he teaches courses in automatic controls and digital controls. His current research interests are in CNC machine tool control technology, advanced process control, magnetic bearing technology, and rotor dynamic and control.

Dr. Lee served as an Editorial Board member of the *International Journal of Precision Engineering and Manufacturing, Chinese Society of Mechanical Engineers*, and *Journal of Applied Mechanics and Engineering*. He is the recipient of the Chinese Society of Engineers Engineering Paper Award (1989), Excellent Research Award (1991–1992) of the National Science Council of Taiwan, Distinguished Research Award (1993–1994, 1995–1996, and 1997–1998) of the National Science Council of Taiwan, Distinguished Engineering Professor Award (1995) of the Chinese Society of Mechanical Engineers, and Distinguished Engineering Professor Award (2001) of the Chinese Institute of Engineers. He was a Research Fellow (1999–2004) of the National Science Council of Taiwan and holds the Chair Professor (2004) of National Chiao-Tung University.